PROCEEDINGS OF SCIENCE

Neutron stars in X-ray binaries as observed by IXPE

Alessandro Di Marco[a,*] **for the IXPE Science Team**[c]

[a] *INAF - Istituto di Astrofisica e Planetologia Spaziali, Via del Fosso del Cavaliere 100, 00133 Rome, Italy*

E-mail: alessandro.dimarco@inaf.it

The Imaging X-ray Polarimetry Explorer (*IXPE*), recently awarded by the American Astronomical Society with the Bruno Rossi prize, during the first 2 years observed several accreting neutron stars in X-ray binaries. Both classical X-ray pulsars, having strong magnetic fields, and weakly magnetized neutron stars, which do not show pulsations, were observed. For the first class, *IXPE* allowed us to determine the geometry of these systems from the polarization properties, but also displayed a more complex scenario with respect to the theoretical predictions. For non-pulsating sources, spectropolarimetry performed with *IXPE* allowed us to model the geometry of the different emitting regions (accretion disk, boundary/spreading layer, accretion disk corona, ...) in a completely novel way. In this proceeding a brief review of these sources and the results obtained by *IXPE* in their observations is reported.

Frontier Research in Astrophysics, IV 09-14 September 2024 Mondello, Palermo, Italy

*Speaker

 ISSN 1824-8039 . Published by SISSA Medialab.

PoS(FRAPWS2024)038

1. Introduction

X-ray binaries (XRBs) include the brightest X-ray sources in the sky, such as Sco X-1. This is the brightest extra-solar X-ray source in the sky and the first discovered [1]. XRBs are systems consisting of a compact object, either a neutron star (NS) or a black hole (BH) and a companion star. Their bright X-ray emission is due to the compact object accreting material from the donor star. Depending on the mass of the donor star, XRBs are conventionally classified into low-mass X-ray binaries (LMXBs) and high-mass X-ray binaries (HMXBs). XRBs display periodic and aperiodic variability; furthermore, both orbital and superorbital modulations in light curves have been observed. About 40% of Galactic XRBs are transient sources due to their large variability, reaching faint luminosities that make them undetectable in typical surveys.

LMXBs have a companion with mass $\lesssim 1 M_\odot$ and they are older than HMXBs (typically 10^9–10^{10} yr); in these systems the compact objects accrete matter from late-type main-sequence stars and white dwarfs by Roche-lobe overflow (RLO). Most LMXBs are discovered in the Galactic center, bulge, and disk, while a substantial fraction are revealed in globular clusters [2]. NSs in LMXBs typically have low magnetic fields ($B \sim 10^8$–10^9 G), and their magnetospheres play a relatively minor role in accretion; thus, the states of BHs and NSs in LMXBs share similarities, being mainly governed by the accretion rate [3]. HMXBs have a massive ($\geq 5 M_\odot$) early-type stellar companion, and they are distinguished from LMXBs in many aspects. They are typically younger ($\sim 10^5$–10^7 yr), and a small number of them were discovered to be associated with supernova remnants, indicating that they are the youngest XRBs and they remain close to their birthplaces (see, *e.g.*, Ref. [4]). Because high-mass stars have powerful stellar winds, direct wind accretion can produce X-ray luminosities in the range $10^{35} - 10^{40}$ erg s^{-1}. Most ultraluminous X-ray sources (ULXs) are thought to be the brightest end of HXMBs in outer galaxies; see *e.g.* Ref. [5]. To date, only a few HMXBs host BHs and candidates, including several wind-fed systems, such as Cyg X-1; the majority are identified to host young NSs with magnetic fields $B \sim 10^{11}$–10^{13} G, because of the detection of X-ray pulsations. Pulsating NSs in XRBs are called accreting X-ray pulsars (XRPs). Unlike weakly magnetized NSs and BHs accreting systems, the accreting processes in XRPs are determined not only by the accretion rate but also by the strong magnetic fields; this results in distinct X-ray emissions and more complicated evolution patterns.

XRBs, being so bright, have been considered ideal candidates for studying X-ray polarization; thus, attempts have been made since the 1970s. In 1975, OSO-8 observed the XRPs Cen X-3 and Her X-1 without significant polarization detection [6] and the LMXB Sco X-1 for which a marginal detection was obtained [7]. Today, the successful launch in December 2021 of the Imaging X-ray polarimetry Explorer (*IXPE*) [8, 9] allowed us to observe several NSs in XRBs and to obtain significant detection of polarization in many of them, opening the possibility to test theoretical models.

In the following, XRBs systems that have NSs as a compact object are presented. NSs are the objects with the highest known density; the matter inside a NS exists in an ultra-dense cold state that cannot be reproduced in any experiment in terrestrial laboratories. The behavior of matter under these conditions is of great interest not only from the astrophysical point of view but also for implications on the physics of fundamental interactions. Studies about the equation of state (EoS) can allow the setting of the mass and radius of the NSs [10, 11], making crucial

astronomical measurements of the NSs radii and masses. In the next sections, X-ray pulsars and weakly magnetized NSs in XRBs are introduced, and *IXPE* results obtained from their observation are reported and discussed for a few of them. In the end, considerations about the results of *IXPE* are reported.

2. Accreting X-ray pulsars

Classical XRPs are sources in which a NS, having a magnetic field up to 10^{13} G, accretes matter from a companion star. Their luminosities are consistently above $\sim 10^{35}$ erg s^{-1} and varying over time by a factor 10–100. XRPs are typically hosted in HMXBs, and their variability is also affected by the interaction of their strong magnetic fields with the matter accreting from the companion, which alters the structure of the accretion flow at the magnetospheric radius, the distance where the magnetic pressure balances the ram pressure in the disk. Thus, the ionized gas from the companion is captured and channeled by the strong magnetic field onto magnetic poles on the NS surface, forming two X-ray hot spots. There, the interaction of matter with the NS releases energy as radiation in a highly anisotropic manner. If rotational and magnetic axes of the NS are misaligned, the observed X-ray radiation becomes pulsed as the NS spins, giving rise to a time-dependent X-ray emission characterizing the XRPs. Therefore, investigating X-ray pulsations provides direct access to the matter motions and X-rays emitted in the very close vicinity of pulsars.

2.1 Classification and properties

All HMXBs exhibit variability and some of them are transient sources. In XRPs, additional variability is introduced by the interaction of the accretion flow with the magnetosphere, which rotates with the same angular velocity as the NS. Different accretion regimes are produced by interactions between the accretion flow and the magnetosphere.

The mass transfer mechanism in most of the classic XRPs is wind accretion (wind-fed) rather than RLO (disk-fed). This is due to the channeling of the material by the magnetic field, so an accretion disk is typically not formed, and the wind accretes matter directly on the magnetic poles. Despite this, some known XRPs are thought to be disk-fed systems where temporary accretion disks can form around the NSs. Accretion disks also tend to form during outbursts in Be XRBs (see below), and it has also been suggested that in some of them an accretion disk may persist while the source is in a quiescent state [12]. In the disk-fed scenario, the magnetic field of the NSs partially penetrates the disk, generating a toroidal magnetic field. Thus, the thickness of the disk affects the size of the hot spots and, consequently, the observed pulse profiles and spectra (see *e.g.*, Refs. [13–15]). Disk-fed XRPs have a steady transfer of material from the donor stars which forms accretion disks; this makes their luminosities persistently high. The same consideration holds for wind-fed systems, where NSs are deeply embedded in strong stellar wind.

Be XRBs are HMXBs having a Be companion with a radius smaller than the Roche lobes and a wide and highly eccentric orbit; the NSs occasionally capture a large flow of matter from the circumstellar decretion disk, triggering transient outbursts. Only a small number of Be XRBs show persistent low luminosities with long spin periods, whereas the majority exhibit transient behavior. The transient Be XRBs exhibit behavior with outbursts, classified as Type I or Type II outbursts. In Be XRBs, a circumstellar decretion disk is ejected from the equator of the Be star

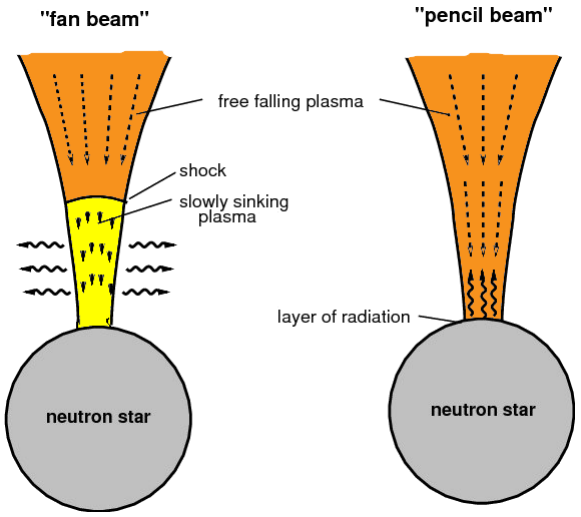

Figure 1: Sketch of the accretion geometries in XRPs: fan beam pattern on the left, pencil beam on the right. Adapted from Ref. [22].

[16]. This disk operates as an inverse accretion disk, transferring outward the angular momentum. NS approaching the periastron passes through this decretion disk and accretion occurs; this regular and quasiperiodic activity is identified as Type I outbursts [17, 18]. They have peak luminosities with an increase of one order of magnitude, and they cover only a small fraction of the orbit. During some Type I outbursts, rapid pulsar spin-up rates are observed, probably due to the formation of an accretion disk [19]. Be XRBs also show much rarer Type II outbursts, the mechanism that produces them is unclear, although they are associated with a highly misaligned and eccentric decretion disk [20]. Type II outbursts are also called giant outbursts because of their much brighter luminosity ($>10^{37}$ erg s^{-1}), and duration lasting for several weeks or even for several orbital periods.

In XRPs, the accretion process and the properties of the emission near the magnetic poles are believed to be strongly dependent on the magnetic field and the luminosity. In particular, for a given magnetic field, when luminosity exceeds a critical value, $L_{crit}\sim10^{37}$ erg s^{-1} [21], a radiation-dominated shock forms above the surface of the NS; below this shock, where the kinetic energy of the infalling matter is significantly reduced, there is a sinking zone called the accretion column. This is an extended region with high energy density, and height positively correlated with luminosity. In this supercritical scenario, the X-ray emission results in a fan beam pattern (see Figure 1-*left*), while in the subcritical accretion regime ($L<L_{crit}$), the radiation pressure cannot fully decelerate the infalling matter. Thus, the matter rapidly decelerates in the atmosphere of the NS, and the radiation is emitted near the NS resulting in a pencil beam pattern (see Figure 1-*right*) with X-rays emitted mainly along the magnetic field lines.

XRPs at luminosity $\geq10^{36}$ erg s^{-1} typically exhibit power-law spectra with an exponential cutoff at energies of approximately 10–20 keV [23]. In some cases a soft X-ray excess is observed, this is often modeled with a blackbody component [12]. XRPs spectra can also display Fe fluorescence emission lines, the most common is Fe Kα and, at times, a component called the 10 keV feature (see Ref. [12] and references therein).

X-ray emission in XRPs originates primarily in regions close to the magnetic poles, where

the electrons in the accretion flow Compton scatter photons produced by a variety of radiative processes [24]; the study of the properties of this emission is fundamental to understanding the physics of plasma accretion and the interaction of radiation with such high magnetic fields (orders of magnitude stronger than the ones achievable in laboratories on Earth). Moreover, the extreme surface magnetic field strength allows quantum effects to take place at the site of emission, affecting the electron scattering cross section. In fact, the electron motion becomes quantized in the direction perpendicular to the magnetic field lines. These quantum effects can lead to a resonance at an energy that is proportional to the magnetic field strength, resulting in absorption line-like features in the XRPs spectra [25]. These absorption lines are called cyclotron resonant scattering features (CRSFs), or simply cyclotron lines, at energy:

$$E_{cyc} \sim \frac{n}{1+z_g} 11.6 B_{12} \text{ keV}, \tag{1}$$

where n is the number of Landau levels, z_g is the gravitational redshift and B_{12} is the NS magnetic field in units of 10^{12} G at poles. Thus, identification of the fundamental ($n = 1$) Cyclotron line represents the most direct way to probe the NS magnetic field on or close to the NS surface. Cyclotron lines also exhibited variations with the accretion luminosity, pulse-phase, and secular time scales; both positive and negative correlations were observed, and, at some time, both trends were observed in the same source. These variations can be exploited to gain insight into the accretion regime: low-luminosity XRPs tend to show a positive correlation, while the negative correlation is more probable for high-luminosity. These two different correlations are supposed to be related to the two different geometries of the subcritical and supercritical regimes.

Further information for XRPs can be obtained by folding data on the basis of the spin period to measure the X-ray pulse profile. Pulse profiles are reported to vary with energy and luminosity. A property of pulse profiles is the pulse fraction: $(I_{max} - I_{min})/(I_{max} + I_{min})$, where I_{max} and I_{min} are the maximum and minimum count rates after background subtraction. For bright XRPs, the pulse fraction tends to increase with energy, even if it has a peculiar behavior near the cyclotron lines. In most cases, the pulse fraction decreases with increasing luminosity. Variations in pulse profile and pulse fraction are thought to be related to the geometry of the accretion flow and its changes with the mass accretion rate. Different beam patterns result in different pulse profiles; in particular, trends in the pulse fraction and pulse profiles with energy and luminosity are consistent with the presence of accretion columns in which the temperature decreases with height, resulting in hard X-rays forming in smaller regions closer to the NS surface [12].

XRPs pulsations can be described with a dipole model with two hot spots. However, the pulse profiles of XRPs are highly structured, showing a great variety from outburst to outburst, and commonly vary with luminosity and photon energy. In some sources, X-ray pulsations show double peaks at high luminosities and a single peak at low luminosities, which can be approximately interpreted as switching between fan beam and pencil beam patterns. Thus, pulse profiles are complex to model because some important factors (*e.g.*, the presence of an accretion disk, the occultation and the reflection by the NS itself, the gravitational light-bending effect, the scattering process by the surrounding matter, the distorted dipole configuration) could modify the pulse shape significantly, leading to asymmetric, narrow spikes, or flare features. Usually, X-ray pulsations in the softer band have a more complex shape and a smaller pulse fraction. Since pulse shapes are

mainly governed by the accretion onto the NS surface, it allows us to estimate the geometry of the magnetic field and beam patterns of emitted X-rays. However, due to the complexity of the radiative process, the dynamical structure of the accretion flow, and the gravitational light bending, it is still theoretically impossible to reproduce pulse profiles at the current stage. On the other hand, once the beam mode switching can be determined, we will be able to estimate the critical luminosity and, thus, to measure the strength of the magnetic field. However, we note that beam patterns at different energy bands could be different, because the magnetized Comptonization cross section is highly energy-dependent. This may lead to a large uncertainty in estimating the critical luminosity according to variations of profile profiles at a narrow energy band.

Thus, the geometrical structure of the emission region in XRPs and the corresponding beam pattern strongly depend on the mass accretion rate; in particular, it depends on the luminosity with respect to the critical luminosity. The study of energy spectra and light curves allows one to extract information about the geometrical configuration of the emitting regions at the NS surface. However, the information is degenerate and modeling is very difficult. The resulting magnetic field geometry, on the other hand, can be cross-checked with polarization observations; these offer an independent tool to investigate the geometry of XRPs.

The radiation from the accretion column is expected to be highly polarized because the Compton scattering cross section is energy and polarization dependent for the energy band below the cyclotron line energy, as well as the vacuum polarization effect during propagation [26]. In fact, considering two normal modes of polarization, the ordinary (O) and the extraordinary (X), these interact in a different way with matter.

Although modeling the polarization degree (PD) in XRPs is a difficult task [27], the polarization angle (PA) was suggested, in Ref. [28], to be modeled with the rotating vector model (RVM) [29, 30]. RVM relates the PA variations along the pulsar phase to the projection of a magnetic dipole in the sky plane. In particular, in the *IXPE* energy range, the magnetic field is expected to be dominated by the dipole component, and the PA is expected to be parallel or orthogonal to its projection onto the plane of the sky, depending on its intrinsic polarization mode. Thus, for radiation dominated by the O-mode the PA is given by [31]:

$$\tan(\mathrm{PA} - \chi_\mathrm{p}) = \frac{-\sin\theta_\mathrm{p}\ \sin\phi}{\sin i_\mathrm{p}\cos\theta_\mathrm{p} - \cos i_\mathrm{p}\sin\theta_\mathrm{p}\cos\phi}, \tag{2}$$

where i_p is the inclination of the pulsar spin with respect to the line of sight, θ_p is the magnetic obliquity, *i.e.*, the angle between the magnetic dipole and the spin axis, ϕ is a phase offset, and χ_p is the position angle measured from north to east of the pulsar angular momentum. In Figure 2, the geometry and examples of the dependency of PA on the spin phase are reported. Obviously, for radiation dominated by X-mode, PA is rotated by 90° with respect to the O-mode.

2.2 IXPE observations of accreting X-ray pulsars

IXPE during the prime mission period, which lasted two years, observed several XRPs, both wind-fed and disk-fed systems, but also Be XRBs and one ULX; some of them were observed a few times in different states. In Table 1, a summary of the observations is reported with reference papers. A high PD value for magnetized NSs was expected in the *IXPE* 2–8 keV energy band for all observed XRPs. Despite this, *IXPE* measured much lower values of PD. For a recent review on

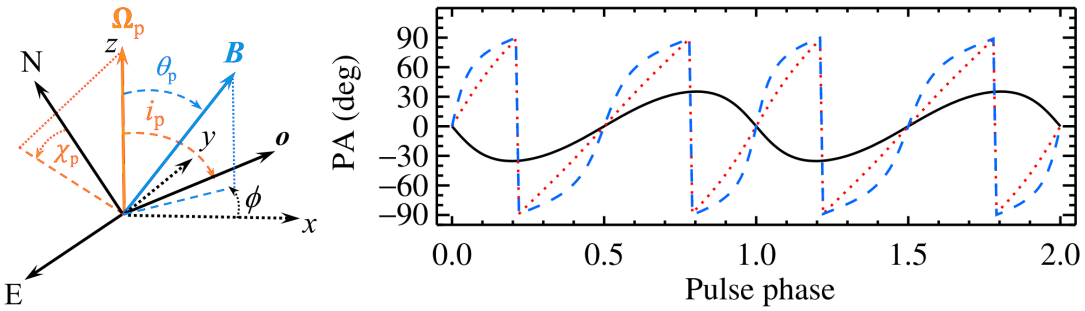

Figure 2: *Left*: geometry of the pulsar reporting main parameters of the RVM. The pulsar angular momentum $\boldsymbol{\Omega}_\mathrm{p}$ is rotated by an angle i_p with respect to the observer $\boldsymbol{o}$; the angle between the magnetic dipole $\boldsymbol{B}$ and the rotation axis is the magnetic obliquity θ_p; the phase ϕ is the azimuthal angle of $\boldsymbol{B}$ in the plane perpendicular to $\boldsymbol{\Omega}_\mathrm{p}$; χ_p is the angle measured counterclockwise between the direction to the north (N) and the projection of $\boldsymbol{\Omega}_\mathrm{p}$ on the plane of the sky (N-E). *Right*: PA as functions of spin phase at different values of i_p and θ_p). Black solid line reports $i_\mathrm{p} = 60°$ and $\theta_\mathrm{p} = 30°$, red dotted line $i_\mathrm{p} = 30°$ and $\theta_\mathrm{p} = 70°$, blue dashed lines $i_\mathrm{p} = 70°$ and $\theta_\mathrm{p} = 85°$. Adapted by Ref. [27].

Name	**Spin Period [s]**	**Luminosity [erg s^{-1}]**	***IXPE* Exp. [ks]**	***IXPE* Reference**
Cen X-3	4.8	1.9×10^{37}	~70 + 180	[32]
Her X-1	1.24	$\sim 3 \times 10^{37}$	$\sim 2 \times 250 + 150$	[33, 34]
4U 1626−67	7.7	6.4×10^{36}	~190	[35]
Vela X-1	283	3.8×10^{35}	~270 + 280	[36]
GRO J1008−57	93.5	$(0.6–1.6) \times 10^{36}$	~85 + 100	[37]
EXO 2030+375	41.31	1.3×10^{36}	~180	[38]
X Persei	837.67	1.2×10^{34}	~ 220	[39]
GX 301−2	696.0	1.3×10^{36}	~290	[40]
LS V +44 17	202.5	$\leq 4 \times 10^{37}$	~130 + 370	[41]
Swift J0243.6+6124	9.87	$(0.6–2.4) \times 10^{37}$	~170 + 70 + 130	[42]
SMC X-1	0.717	2×10^{38}	~320	[43]

Table 1: List of XRPs observed by *IXPE* and their parameters. X-ray luminosities during *IXPE* observations are reported as indicated in Ref. [27].

X-ray polarization and the results of the *IXPE* observations of XRPs during the first two years of operations, see Ref. [27].

IXPE observations of XRPs started with Cen X-3 and Her X-1 (see Sect. 2.2.1). Cen X-3 was observed twice; in the first observation, no significant detection was obtained. Combining data from the two observations, having an average luminosity near the critical one, the most striking result was a rather low PD: 5.8 ± 0.3% [32]. When data were divided into spin-phase bins, a significant variation of polarization was discovered, with an anti-correlation of PD with the pulse profile and maximum PD~15%. The anti-correlation observed is compatible with the expectations for subcritical XRPs reported in Ref. [28], but the PD values are lower than the predictions. The RVM model allowed one to determine the position angle and magnetic obliquity of about 49° and

17°, respectively [32].

The capabilities of *IXPE* make it possible to study polarization as a function of energy; XRPs observed by *IXPE* do not show a significant dependence of PD and/or PA on energy, except for a few cases, such as Vela X-1 (see Sect. 2.3) and X Persei. The latter has an average polarization compatible with zero, but PD increases from ∼0% up to ∼30% going from 2 to 8 keV [39], and when the data are divided into phase bins, a significant variation of polarization is observed, even if with a pattern opposite to Cen X-3 (PD is correlated with flux). The RVM, when applied, allowed us to measure a magnetic obliquity close to 90°, making X Persei an orthogonal rotator.

IXPE observed also the two Be XRBs GRO J1008−57 and LS V +44 17, the latter is presented in Sect. 2.4. Both were observed more times as a function of the luminosities. GRO J1008−57 was observed twice during the outburst of November 2022 [37] with luminosities that differed only by a factor of ∼2. The polarimetric properties of the two observations were almost identical. Combining the two observations and applying the RVM, a highly significant measure of the geometrical parameters was obtained. The results showed a positive correlation of PD with the pulsed profile and large magnetic obliquity (∼75°), similarly to X Persei, but no significant variation of polarization with energy is reported.

SMC X-1 is the only extragalactic XRP observed by *IXPE*; three pointings were made that covered a significant fraction of its ∼45 d superorbital cycle [43]. The source showed very high luminosity during the *IXPE* observations (see Table 1), making it the most luminous XRP observed. Although SMC X-1 was clearly in the supercritical regime, the polarization properties resulted to be very similar to the ones observed from Cen X-3 [36].

In the summer of 2023, the ULX X-ray pulsar Swift J0243.6+6124 went to the outburst and *IXPE* observed it three times [42]. This XRP showed variations in the polarimetric properties, but not as extreme as in LS V +44 17.

IXPE also observed objects where the counting statistics did not allow for a detailed analysis, such as GX 301−2 [40] or EXO 2030+375 [38], where polarization was significant only in a few phase bins. Although the observed PD was lower than expected in all XRPs, it was detected significantly in at least the phase-resolved data. The only exception is 4U 1626−67 [35].

2.2.1 Her X-1

Her X-1 was observed several times by *IXPE* during the first two years of operations, with the aim of studying the polarization of this system along its 35 d super-orbital periodicity presumably related to the precession of the NS [45]. *IXPE* performed observations of Her X-1 in the so-called "main-on" and "short-on" states. The geometrical parameters of the NS were determined using RVM. Combining X-ray and optical polarimetric data, a ∼20° misalignment of the NS spin axis and the angular momentum of the binary orbit was reported [33]. In addition, a variability of PA was revealed during the superorbital cycle, see Figure 3 [34, 44]. In Ref. [34], a detailed modeling of the pulse-phase-resolved data at different superorbital phases was used to point out that the Her X-1 superorbital cycle is due to free precession of the NS crust; indications that the NS geometry is altered by torques were also found. This result shows the potentiality of polarimetric data, which allowed us for the first time to measure the geometry of this source and to monitor it along the superorbital period confirming the presence of a precession.

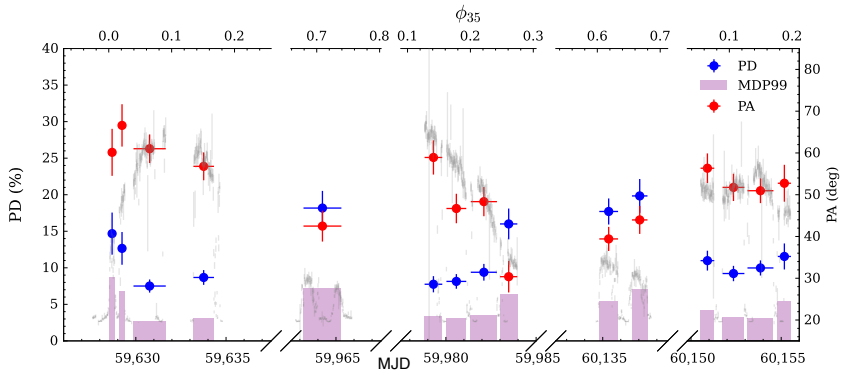

Figure 3: Her X-1 PD (blue, left axis) and PA (red, right axis) as measured along time and superorbital phase (upper axis). The minimum detectable polarization at 99% CL is reported in pink, while the flux behavior is reported in shaded gray. Figure from Ref [44].

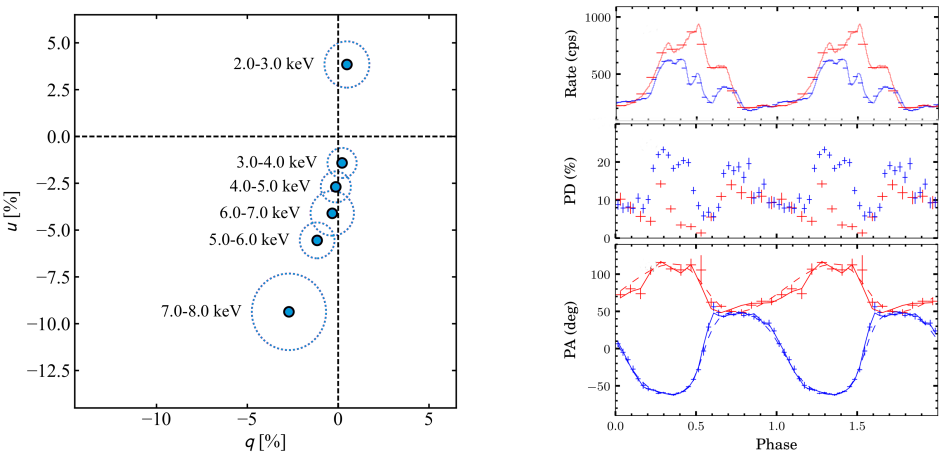

Figure 4: *Left*: Polarization as a function of energy in Vela X-1, adapted by Ref. [36]. *Right*: form top to bottom the pulse-phase dependence of the flux, the PD and the PA (lines report RVM best-fit model) of LS V +44 17 for the first (red) and second (blue) *IXPE* observations, respectively. Adapted by Ref. [41].

2.3 Vela X-1

Vela X-1 is the prototype of wind-fed XRPs, it was observed by *IXPE* twice. During the first observation, which lasted a long time during the eclipse, no high significant detection of polarization was reported; the two observations showed compatible polarimetric properties, allowing for a combined analysis which permitted us to obtain a significant detection of polarization. The most peculiar result in this source is the energy dependence of the polarimetric properties; see Figure 4-*Left*. At lower energies, the PD value decreases with energy, reaching a minimum around ~3.5 keV, then starts to increase, reaching around 10% at 8 keV [36]. Moreover, the PA makes a 90° swing between low and high energies, similar to what was expected and observed for weakly magnetized NSs such as 4U 1820−30. This result, combined with a very complex pulse profile shape, results in very complicated phase-resolved variations of the PA, which cannot be fitted with the RVM leaving Vela X-1 an XRP with still unknown geometry.

2.4 LS V +44 17/RX J0440.9+4431

LS V +44 17 is a transient Be XRB, initially suggested as persistent [46]. During its last outburst at the beginning of 2023, *IXPE* made two observations. The pulse profile showed variations; see the top panel of Figure 4-*Right*, and the PD grew from less than 10% to more than 15%, see the middle panel in the same Figure, when the flux decreased. The most serendipitous result was obtained from PA, which changed dramatically between the two observations; see the bottom panel in Figure 4-*Right*. The RVM fits the PA phase dependence rather well in both cases, and the parameters resulted in being highly different with the pulsar inclination and magnetic obliquity changing by ∼40° and ∼30°, respectively, while $\chi_{\rm p}$ rotated by ∼90°. Even if the $\chi_{\rm p}$ change could be related to a switch between modes and magnetic obliquity with an evolution of the hot spots, the strong variation of the inclination on a short time scale is very difficult to believe. Thus, an alternative idea was proposed based on the presence of two polarized components: a constant term that does not depend on the pulse-phase and a pulse-phase dependent one described by the RVM. In this scenario, the best fit of the constant component results in a polarized flux of 3–4.5% the pulse-average flux, depending on the observation, while the PA was found to be consistent with the optical PA in LS V +44 17 [41]. This result can be interpreted as evidence in favor of an accretion disk being responsible for the constant polarized component. The RVM applied to PA for the pulsed component resulted in a pulsar spin rotated by ∼75° (or ∼15° in X-mode radiation dominated) from the constant one, possibly implying a misalignment between the pulsar spin and the orbital axes.

3. Weakly magnetized Neutron Stars in X-ray binaries

IXPE, during the prime mission period, observed several classes of sources; considering that this is a discovery mission, the ideal targets were bright X-ray sources such as LMXBs. NSs hosted in LMXBs are typically very bright sources which include Sco X-1, the brightest X-ray source in the sky. These are systems studied since the birth of X-ray astronomy, but for which several open questions are still open due to model degeneracy, as explained in the following.

3.1 Classification and properties

LMXBs are bright X-ray sources; typically when they host a NS, this owns a weak magnetic field ($B \sim 10^8$–10^9 G) and it accretes matter via RLO from a stellar companion having a mass smaller than the solar mass [47]. Although WMNSs do not show pulsations, they can show quasi-periodic oscillations (QPOs) in the Hz and kHz ranges that can help, as their spectral hardness, classify them [48]. The classification of WMNSs is based on the shape of their tracks in the X-ray hard color/soft color diagram (CCD) or hard color/intensity diagram (HID) [48, 49]. Two main classes have been identified: (i) Z sources have luminosities $>10^{37}$ erg/s (near-Eddington X-ray luminosities) and exhibit a Z-like shape in the CCD/HID made of three distinct branches (horizontal, normal, and flaring branches in order of hardness, respectively); (ii) atoll sources have luminosities 10^{36}–10^{37} erg/s and show in the CCD/HID a single rounded spot having a harder spectrum, which defines the island state, plus a banana-like shape having a softer spectrum, that can be divided on the basis of their increasing luminosity into left-lower (LLB), lower (LB), and upper banana (UB). Z sources can be further classified into the following categories: Cyg-like,

where the full Z is tracked on the CCD/HID, and having higher inclinations; Sco-like, having lower inclination and with an almost missing horizontal branch. Moreover, accretion in these systems can be persistent or go through periods of accretion activity and quiescence, where accretion is almost absent. Furthermore, transient WMNSs XTE J1701-462 [50], and 1A 1744-361 [51] have shown a switch from atoll-like to Z-like behavior over the course of the same outburst, as the mass accretion rate changes. Short spin periods (milliseconds), expected to characterize LMXBs, have been detected only from a few atoll sources [52].

Spectral and timing properties, apart from classification, provide clues about the emission mechanisms. Several spectral models have been proposed in the last 40 years to describe the relative contribution in the different states due to: the accretion disk [53]; the NS surface; the region where the inflow material meets the surface of the NS named boundary layer (BL) [54, 55] or the gas layer that extends up to high latitude on the surface of the NS called spreading layer (SL) [56, 57]; the possible presence of a corona [58].

Transient WMNSs can exhibit very hard spectral states at the beginning of an outburst [59, 60]. In these hard states, the spectra are dominated by a hard Comptonized component, probably coming from an accretion disk corona (ADC), and a soft thermal component associated with emission from the NS surface or BL/SL or the inner accretion disk. On the other hand, spectra of WMNSs in a softer state are dominated by emission from the accretion disk near the NS with weakly Comptonized radiation. Two historical models were proposed to describe the continuum of these spectra: the eastern model [61] using a soft multi-color disk blackbody for the emission of the accretion disk in combination with a hard Comptonized single-temperature blackbody component; the western model [62], uses a soft single-temperature blackbody to model emission from the NS or the BL/SL with a hard Comptonized accretion disk component. In Ref. [63], a new hybrid model was proposed to build a coherent view of the spectral evolution between the different states in two transient atolls. In this hybrid model, other than a weak Comptonized component that is accounted for by a power-law component, the soft state assumes two thermal components, one for the accretion disk with a multi-color blackbody and one with a single-temperature blackbody to describe NS or SL/BL emissions. All of those different models for the continuum are degenerate from a spectral point of view, but the spectral analysis of QPOs revealed that the strongest variability is associated with a hard spectral component that originates close to the surface of the NS, favoring the eastern model scenario [64–66].

In addition to the continuum, in WMNSs, photons reprocessed from the accretion disk form a further spectral component known as the reflection spectrum [67–70]; this latter is characterized by emission and absorption lines having characteristics indicative of the physical properties of the material in the disk (*e.g.*, composition, ionization state, density, etc.). The main features of the reflection are a Compton back-scattering hump [71–73] and a Fe emission line complex at ~6.4 keV. As reported, *e. g.*, in Ref. [74], modeling the Fe line profile enables a measurement of the inner disk radius and of the inclination of the system. For NSs, the inner disk radius estimate can provide an upper limit on the NS radius impacting studies of the equation of state of ultra-dense, cold matter, and extent of the BL region extending from the surface of the NS, and on the amplitude of the magnetic field in these systems.

IXPE, thanks to its unique capabilities, gives the opportunity to use X-ray polarization, in addition to spectral and timing information, to disentangle these degenerate models. In particular,

the exact geometry of the region between the inner disk, the NS surface, and the corona remains a subject of debate [75]. Thus, X-ray polarization, which is strongly dependent on the geometry of the emission regions, can allow for a deeper understanding of these systems. In fact, the polarization vectors in systems with BL/SL aligned to the disk symmetry axis are expected to be ~90° apart or parallel, depending on the geometry and optical depth of the BL/SL represented by the Comptonized spectral component [76–78]. Thus, spectropolarimetric analysis can allow one to determine the geometry of the emission regions by studying the PA associated to the soft and hard components.

3.2 IXPE observations of Weakly Magnetized Neutron Stars

During its first two years of operations, *IXPE* observed several WMNSs; in particular, it observed three Z sources, four atoll sources, two peculiar sources, and one transient source exhibiting a Z-like behavior. The persistent Z sources observed by *IXPE* were Sco X-1 [79], the only Sco-like source, and the two Cyg-like: Cyg X-2 [80], and GX 5−1 [81]. Among the atoll sources, *IXPE* observed GS 1826−238 [82], GX 9+9 [83], 4U 1624−49 [84], and the ultra-compact X-ray binary (UCXB) 4U 1820−30 [85]. *IXPE* also observed the youngest known XRB Cir X-1 [86], and the peculiar source GX 13+1 showing intermediate behavior between the Z and the atoll sources [87], the latter was observed during the first *IXPE* Guest Observer proposals period further two times [78, 88]. The only transient WMNS observed by *IXPE* was XTE J1701−462 [89], which in the past has shown atoll and Z behaviors, but during *IXPE* observations it was observed along two Z branches.

Cyg X-2 was the first Z source observed by *IXPE*. The state of the source, during the observation, was reported to be probably in the upper part of the Normal Branch (NB). A high significant detection of polarization was reported in the 2–8 keV energy band 1.9%±0.3% at −40°±4° [80]. An indication of an energy-dependent PD was reported: in the 2–4 keV the measured PD was 1.5% ± 0.3% with PA=−36° ± 5°, and 2.8% ± 0.6% at −46° ± 6° in the 4–8 keV band. PA was reported to be aligned with the direction of the measured radio jet ∼ − 39° [90], *i.e.*, orthogonal to the disk. In September 2022, *IXPE* observed XTE J1701−462 during its outburst twice [89]; this source was previously reported to show both Z and atoll behaviors [50], but during the two *IXPE* observations it was in the horizontal branch (HB) and in the NB, respectively. In the HB an average PD 4.6% ± 0.4% at PA=−38° ± 2° was measured, while in the NB only an upper limit for PD<1.5% was set at 90% CL [89]. Recently, an indication of a rotation of the PA was reported for the NB of XTE J1701−462 [91, 92]. This observation showed for the first time a variation in polarization along the Z track. The result obtained for XTE J1701−462 has been confirmed for the persistent bright Cyg-like source GX 5−1 [81]. In two short snapshots, *IXPE* observed the source along the whole Z pattern. In the first snapshot, the source was in HB and a degree of polarization of 4.3% ± 0.3% at PA −10° ± 2° was measured, while in the second observation the source went into the NB and the flaring branch (FB), the statistic did not allow for a disentanglement of the polarization in the two states, and the polarization for the NB+FB states resulted in 2.0% ± 0.3% at PA= −9° ± 4°.

The only Sco-like source observed by *IXPE* during the prime mission period was Sco X-1. As reported in Ref. [79], a significant polarization degree of 1.0% ± 0.2% and a polarization angle of 8° ± 6° at 90% CL are measured. The source during the *IXPE* observation was in the Soft Apex (SA) state, connecting the FB to the NB. During observation, no significant evidence for a variation in PD between FB and SA was reported. The measured PA results appear to be not aligned with

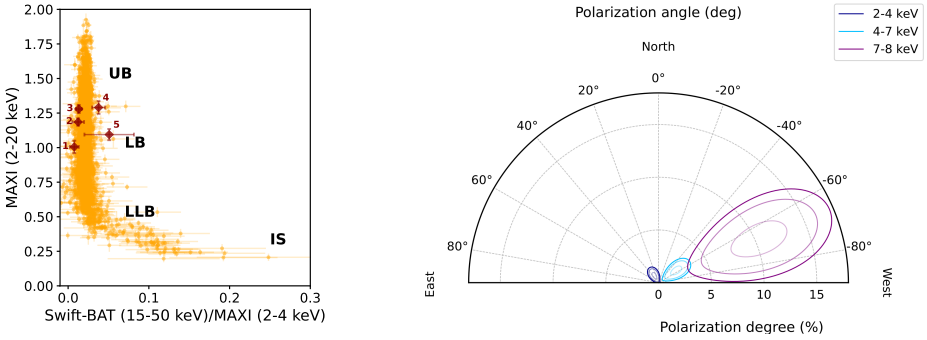

Figure 5: *Left*: HID with different states of the source identified: island state (IS), Upper (UB), Lower (LB), and Left Lower (LLB) Banana. The red points mark the source state during the observative campaign (see [85] for details on this). *Right*: X-ray polarization in 4U 1820−30 in the three energy bins 2–4, 4–7, and 7–8 keV; contours correspond to 50%, 95%, and 99% CL. Plots adapted by Refs. [85, 92].

the radio jet direction position angle [93], nor with the previous low significant measurement of polarization from OSO-8 [94] and PolarLight [95].

GS 1826−238 was the first atoll source observed by *IXPE* [82] and is the only WMNS for which no significant detection of polarization has been reported. In particular, the degree of polarization is <1.3% at 99.73% CL in the 2–8 keV energy band, and no clue of polarization variability with energy was observed [82]. The second atoll source observed by *IXPE* was GX 9+9, for which a significant average polarization was measured in the 2–8 keV energy band: PD = 1.4% ± 0.3% at PA = 68° ± 6° [83]. An energy resolved analysis was performed, obtaining an indication that PD increases with energy. The dipping source 4U 1624−49 was observed by *IXPE* in August 2023, measuring a polarization of 3.1% ± 0.7% at 81° ± 6° in the 2–8 keV energy band [84]. An indication of a dependency of PD with energy is reported with values 1.6% ± 0.8%, 2.9% ± 0.9%, and 6% ± 2% in the energy bins of 2–4, 4–6, and 6– 8 keV, respectively. The PA is almost constant in the same energy bins. In the light curve of 4U 1624−49 narrow dips are visible, but they were too short to allow a study of the polarization in these dips. *IXPE* observed a further atoll source, the Ultra-compact 4U 1820−30 which results are reported in Sect. 3.3.

In addition to the previous sources, *IXPE* observed two other peculiar sources, Cir X-1, which is a Be XRB that has the same behavior as WMNSs and GX 13+1 that has a not clear classification. The results of Cir X-1 and GX 13+1 are reported in Sect. 3.4 and Sect.3.5, respectively.

3.3 4U 1820-303

4U 1820−30 is the UCXB with the shortest orbital period (~685 s) having a He white dwarf companion; this system is considered the first identified source of Type-I X-ray bursts. Its time evolution along the banana and island states is slow and follows a ~170 d superorbital period.

IXPE observed 4U 1820−30 in two different joint observative campaigns. Both observations were performed when the source was in the LB state (see Figure 5–*left*), allowing for a combined analysis of the two data sets [85].

Although 4U 1820−30 has a not significant polarization in the 2–8 keV energy band, it has a measured PD strongly depending on the energy, as reported in Figure 5–*right*; the degree of

polarization increases up to $10.3\% \pm 2.4\%$ in the 7–8 keV energy band, and the angle of polarization varies from $30° \pm 11°$ in the 2–4 keV energy band to $-67° \pm 7°$ in the 7–8 keV. The result obtained by *IXPE* for 4U 1820−30 cannot be explained with polarimetric models for BL/SL and a possible explanation could be the presence of a reflection component; considering the relative fluxes, the reflection cannot fully explain the observed energy dependence of polarization [85], neither the ∼90° rotation of the PA.

A possible explanation for the result is some geometry that is not standard, such as the one reported in Ref. [96]. To achieve such a high PD with strong energy dependence, slab-like corona geometry could be invoked. About the 90° variation of PA with energy, this can be expected in case the NS axis is well aligned with the disk, or by a variation of the optical thickness of the slab.

3.4 Cir X-1

Cir X-1 is a young Be XRB, initially suspected to host a black hole, based on its spectrum, but then Type I X-ray burst observations undoubtedly indicated the presence of a NS [97]. Cir X-1 has an eccentric orbit, causing its flux and spectrum change significantly over the ∼16.5 d orbital cycle, and even if the companion is suggested to be a massive Be, its behavior is typical of WMNSs. Flux variations along the orbital period are characterized by a dip followed by a flaring phase; this regular flux modulation in the X-ray is suggested to be related to variations in the mass accretion rate along the eccentric orbit [98]. Thus, Cir X-1 is a very peculiar source that showed signatures of both Z and atoll sources, making its classification not standard [99].

Cir X-1 is one of the few NS in XRBs for which radio jets have been spatially resolved, and this source also showed X-ray jets that were almost aligned with radio jets [100, 101]. These X-ray jets indicate the ejection of matter at relativistic speeds; this is noteworthy for comparing NS systems with BHs, as it shows that jets can be launched without the involvement of the Blandford-Znajek mechanism [102]. Recently, the orientation of radio jets has been observed to vary over time, probably due to the precession of the emitting regions, which are widely accepted to be near the compact object, or due to interactions with interstellar matter [103].

IXPE observed Cir X-1 in two different periods (total exposure time 263 ks): the first covered the transition from dip to flaring and the flaring itself, the second covered a stable phase before the dip (see Figure 6–*Left*). As reported in Figure 6, *IXPE* measured a non-significant polarization during the transition from dip to flaring, while a significant rotation of the PA between the flaring and stable phases is observed. Data have also been analyzed in terms of hardness ratio, obtaining that the PA is orthogonal with the radio jet (parallel to the disk) when the source is softer, while the PA approaches the radio jet direction when it is harder, but never aligns with it.

Those results can be explained by an emission dominated by the disk and/or the BL at high accretion rates when the flux is higher (PA aligned with the accretion disk and orthogonal to the radio jet), while the SL became dominant at lower fluxes/accretion rates, and PA results to be parallel with the NS axis, which should be aligned with the radio jet. The fact that when the flux is harder, it does not perfectly align with the direction of the radio jet could indicate relativistic effects that can cause a PA rotation, a possible precession, or a misalignment of the NS axis with respect to the disk axis [86]. The eccentric orbit of Cir X-1 can be the result of a significant supernova kick, which leads to a misalignment of the NS rotation axis and the newly formed binary orbit. Young NS, as suggested for the case of Cir X-1 from the detection in its surroundings of an extended emission of a

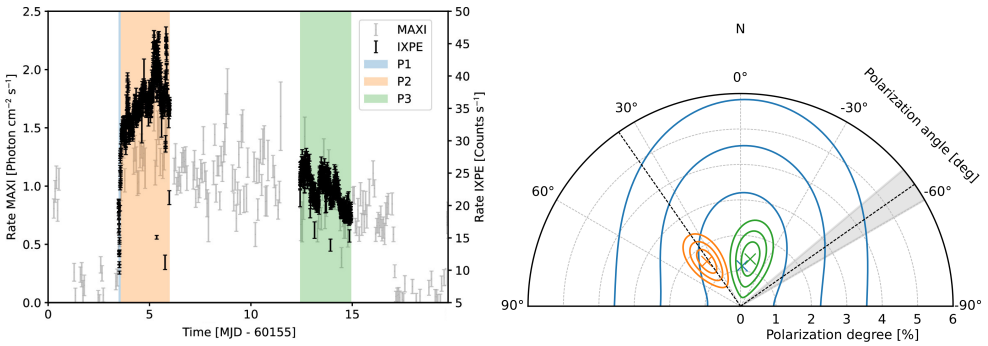

Figure 6: *Left*: time evolution of the Cir X-1 rate by MAXI (2–20 keV) and *IXPE*, adapted from [86]. *Right*: polarization in the entire *IXPE* energy band, adapted from [86], for the same time intervals and with same color code reported in the *left* panel. The shaded region indicates the direction of the radio jet within uncertainties, while the black lines indicate the same direction and its orthogonal direction where the disk polarization is expected to lie. Contours report the 68%, 95%, and 99% CL intervals.

supernova remnant, had not yet enough time to accrete material, so that its spin axis aligns with the one of the disk; such a misalignment would imprint observable signatures in the X-ray polarimetric data.

3.5 GX 13+1

GX 13+1 is a persistent and peculiar LMXB classified as a bright atoll source [49] or a Z source that showed peculiar features [70]. Because of this, it was found that identifying the state of GX 13+1 was more difficult than in other WMNSs. Furthermore, GX 13+1 has a high-inclination (60°-80°) with the presence of periodic (every ∼24.5 d) [104, 105] and aperiodic dips [87, 88, 106]; no evidence of eclipses is observed in the light curve [104].

IXPE observed GX 13+1 three times [78, 87, 88] reporting in all of them a significant polarization in 2–8 keV with a high variability of polarization with time. A very intriguing result obtained for this source is the presence of a ∼70° continuous rotation of the PA only during the first observation, where a dip is also observed [87], see Figure 7–*left*. The polarization measured for the dip is 7.5% ± 1.7% at −51° ± 7°, which is higher than the average polarization. This rotation has recently been reported, although with lower significance, for XTE J1701−462 [91, 92].

This continuous rotation was not observed during the second *IXPE* observation [78]. The PD variations observed in these first two observations were explained in terms of two polarized components: the BL/SL and the wind. One of the two components must have constant PD and the second can vary with time. For example, for a wind constant polarization, the variation of polarization could be due to BL/SL different geometries, whereas for variations related to the wind component, these could be related to different optical depths of the wind along the line of sight between the source and the observer.

During the third *IXPE* observation, two dips are reported, and, even if no continuous rotation was observed, evidence of PA variation is reported during these two dips [88]. Combining the results from the three *IXPE* observations in Ref. [88], the evidence is obtained for a polarization dependent on the flux and hardness ratio; in particular, the PD and PA trends are related to the dips.

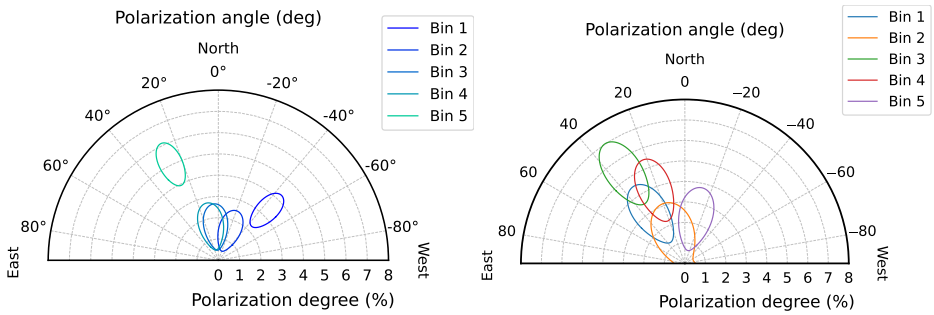

Figure 7: Time dependence of the PD and PA dividing the first (*Left*) and the second (*Right*) *IXPE* observations into five equal time bins. Confidence regions are reported at 68% CL. Adapted from Refs. [78, 87].

This result can be explained with a wind component, but it could also be explained as evidence for the presence of an extended accretion disk corona [88].

4. Conclusion

IXPE observed several accreting NSs in XRBs during its first two years of operation. This class of sources, both pulsating and non-pulsating, given their high luminosities, are ideal candidates to perform polarimetric studies. *IXPE* provided the first opportunity to test the existing theoretical models for accreting NSs with high significance. In the case of XRPs, *IXPE* measured a PD significantly lower (PD below 20%) than theoretical predictions (PD up to 80%). This inconsistency has been discussed in different papers. A possible explanation could be a mixing of different emission components (as reported, *e.g.* in Ref. [32]) having different polarimetric properties producing a low average PD. In addition, simultaneous observations of emissions from the two hot spots at different angles could result in a combined emission with a low PD value. A further possible explanation, given, for example, in Ref. [33], is that low PD is related to the structure of the NS atmosphere; in particular, if the vacuum resonance occurs in a transition atmospheric layer having a sharp temperature gradient, low PD values can be obtained. For very bright XRPs ($\gtrsim 10^{38}$ erg s^{-1}), in Refs. [27, 43] was supposed that an optically thick envelope can intercept a substantial fraction of the emission from the NS producing a depolarization.

Even if PD is lower than expectations, the polarimetric data of the XRPs fitted very well with the RVM. The application of the RVM to PA variations along the pulse-phase allowed us to constrain the geometrical parameters of all observed XRPS, except Vela X-1 [36] and 4U 1626−67 [35]. The geometrical parameters sometimes resulted to vary with time, as in the case of Her X-1, where the variations have been explained by precession [34, 44]. For LS V +44 17 the variations of the geometrical parameters were too large and an alternative model that includes a non-pulsed polarized component has been proposed and successfully applied to explain the result [41]. This model also describes the Swift J0243.6+6124 data quite well [42]. Thus, applying the RVM to independently determine the geometrical configuration of XRPs allowed for the first time to break the degeneracy between the geometry of the pulsar and the physics of its emission.

IXPE also observed non-pulsating NSs, both Z and atoll sources, which showed polarimetric properties that varied with accretion rate and/or hardness [81, 86, 88, 89]. In particular, for Z sources, a higher PD is measured in HB (∼4%), compared to that in the NB/FB (≤2%). In [79], for Sco X-1 an attempt was made to measure polarization in flaring and no flaring, but no evidence at 90% CL for a different polarization is observed. Theoretical models predicted for these systems a polarization aligned with the accretion disk axis, *i.e.* parallel to the radio jet or normal to it. In fact, polarimetric models for WMNSs the geometrical models of the different components (disk, BL, and SL) are assumed to be slabs with a polarized emission in the plane of the slab or orthogonal to it, depending on the optical depth. Thus, a comparison of the PA and the direction of the radio jet allows us to study the geometry of these systems. *IXPE* observed three sources for which the radio jet has been spatially resolved: Cyg X-2 [90], Sco X-1 [93] and Cir X-1 [100]. In Cyg X-2, the PA is aligned with the radio jet, while Sco X-1 and Cir X-1 are not aligned with it. Moreover, in Sco X-1, the PA does not align with previous measurements by OSO-8 [94] and PolarLight [95]. In Cir X-1, the PA results vary in time along the orbit and with the hardness ratio. These results could suggest the presence of a disk precession or a variation of the geometry with the source state/accretion rate.

IXPE results also showed that the average polarization in 2–8 keV measured for the atoll sources is lower than in the Z sources with atoll sources GX 9+9, 4U 1624−49 and 4U 1820−30 displaying an energy-dependent polarization [83–85]. Spectropolarimetric analysis assigning polarization to the disk and the Comptonized component displayed PA not always 90°apart as expected from models for aligned systems; these results, joint with the comparison with the radio jet direction, show a more complex scenario than the simple presence of disk and SL/BL; further components such as ADC, wind or reflection need to be included.

IXPE observed two dipping sources: 4U 1624−49 and GX 13+1. Only for GX 13+1 the polarization was measured during the dips [87, 88], and recently a paper on this was published [88]. Until now, two sources have shown a PA rotation along one observation: GX 13+1 [87] and XTE J1701−462 [91]. The rotation was observed only in the first observation of GX 13+1, and in the NB of XTE J1701−462, while in the other observations of these sources no continuous rotation has been reported.

In conclusion, *IXPE* observations of accreting NSs in XRBs displayed a behavior much more complex than the theoretical predictions. The increasing number of observations and results contribute to better understanding their behavior, especially when more observations of the same target were made. As an example, Swift J0243.6+6124 and LS V +44 17 multiple observations allowed us to point out the presence of a non-pulsating polarized component, while WMNSs observations in different states allowed us to display PD variations with hardness/accretion. In the case of GX 13+1, the three observations, which also included dips, are helping to characterize and better understand the contribution from the wind and/or an accretion disk corona. Thus, *IXPE* and X-ray polarimetry greatly improve our understanding of these systems.

Acknowledgments

This research used data products provided by the IXPE Team (MSFC, SSDC, INAF, and INFN) and distributed with additional software tools by the High-Energy Astrophysics Science Archive Research Center (HEASARC), at NASA Goddard Space Flight Center (GSFC). IXPE is a joint US

and Italian mission. ADM is supported by the Italian Space Agency (Agenzia Spaziale Italiana, ASI) through the contract ASI-INAF-2022-19-HH.0 and partially by MAECI with grant CN24GR08 "GRBXRP: Guangxi-Rome Bilateral Agreement for X-ray Polarimetry in Astrophysics".

References

[1] R. Giacconi, H. Gursky, F.R. Paolini and B.B. Rossi, *Evidence for x Rays From Sources Outside the Solar System*, Phys. Rev. Lett. **9** (1962) 439.

[2] H.J. Grimm, M. Gilfanov and R. Sunyaev, *The Milky Way in X-rays for an outside observer. Log(N)-Log(S) and luminosity function of X-ray binaries from RXTE/ASM data*, *Astron. Astrophys.* **391** (2002) 923 [astro-ph/0109239].

[3] C. Done, M. Gierliński and A. Kubota, *Modelling the behaviour of accretion flows in X-ray binaries. Everything you always wanted to know about accretion but were afraid to ask*, *Astron. Astrophys. Rev.* **15** (2007) 1 [0708.0148].

[4] V. Hénault-Brunet, L.M. Oskinova, M.A. Guerrero, W. Sun, Y.H. Chu, C.J. Evans et al., *Discovery of a Be/X-ray pulsar binary and associated supernova remnant in the Wing of the Small Magellanic Cloud*, *Mon. Not. R. Astron. Soc.* **420** (2012) L13 [1110.6404].

[5] A. King, J.-P. Lasota and M. Middleton, *Ultraluminous X-ray sources*, *New A Rev.* **96** (2023) 101672 [2302.10605].

[6] E.H. Silver, M.C. Weisskopf, H.L. Kestenbaum, K.S. Long, R. Novick and R.S. Wolff, *The first search for X-ray polarization in the Centaurus X-3 and Hercules X-1 pulsars.*, *Astrophys. J.* **232** (1979) 248.

[7] K.S. Long, G.A. Chanan, W.H.M. Ku and R. Novick, *The linear X-ray polarization of Scorpius X-1.*, *Astrophys. J. Lett.* **232** (1979) L107.

[8] P. Soffitta, L. Baldini, R. Bellazzini, E. Costa, L. Latronico, F. Muleri et al., *The Instrument of the Imaging X-Ray Polarimetry Explorer*, *Astron. J.* **162** (2021) 208 [2108.00284].

[9] M.C. Weisskopf, P. Soffitta, L. Baldini, B.D. Ramsey, S.L. O'Dell, R.W. Romani et al., *The Imaging X-Ray Polarimetry Explorer (IXPE): Pre-Launch*, *JATIS* **8** (2022) 026002 [2112.01269].

[10] R.C. Tolman, *Static solutions of einstein's field equations for spheres of fluid*, *Phys. Rev.* **55** (1939) 364.

[11] J.R. Oppenheimer and G.M. Volkoff, *On massive neutron cores*, *Phys. Rev.* **55** (1939) 374.

[12] A. Mushtukov and S. Tsygankov, *Accreting Strongly Magnetized Neutron Stars: X-ray Pulsars*, in *Handbook of X-ray and Gamma-ray Astrophysics*, p. 138 (2023), DOI.

[13] V. Doroshenko, S.N. Zhang, A. Santangelo, L. Ji, S. Tsygankov, A. Mushtukov et al., *Hot disc of the Swift J0243.6+6124 revealed by Insight-HXMT*, *Mon. Not. R. Astron. Soc.* **491** (2020) 1857 [1909.12614].

[14] L. Ji, V. Doroshenko, A. Santangelo, C. Güngör, S. Zhang, L. Ducci et al., *Timing analysis of 2S 1417-624 observed with NICER and Insight-HXMT*, *Mon. Not. R. Astron. Soc.* **491** (2020) 1851 [1910.03955].

[15] L.D. Kong, S. Zhang, Y.P. Chen, S.N. Zhang, L. Ji, V. Doroshenko et al., *Two Complete Spectral Transitions of Swift J0243.6+6124 Observed by Insight-HXMT*, *Astrophys. J.* **902** (2020) 18.

[16] T. Rivinius, A.C. Carciofi and C. Martayan, *Classical Be stars. Rapidly rotating B stars with viscous Keplerian decretion disks*, *Astron. Astrophys. Rev.* **21** (2013) 69 [1310.3962].

[17] A.T. Okazaki and I. Negueruela, *A natural explanation for periodic X-ray outbursts in Be/X-ray binaries*, *Astron. Astrophys.* **377** (2001) 161 [astro-ph/0108037].

[18] A.T. Okazaki, K. Hayasaki and Y. Moritani, *Origin of Two Types of X-Ray Outbursts in Be/X-Ray Binaries. I. Accretion Scenarios*, *Publ. Astron. Soc. Jpn.* **65** (2013) 41 [1211.5225].

[19] J. Ziolkowski, *Be/X-ray binaries.*, Mem. Soc. Astron. Italiana **73** (2002) 1038 [astro-ph/0208455].

[20] R.G. Martin, C. Nixon, P.J. Armitage, S.H. Lubow and D.J. Price, *Giant Outbursts in Be/X-Ray Binaries*, *Astrophys. J. Lett.* **790** (2014) L34 [1407.5676].

[21] A.A. Mushtukov, V.F. Suleimanov, S.S. Tsygankov and J. Poutanen, *The critical accretion luminosity for magnetized neutron stars*, *Monthly Notices of the Royal Astronomical Society* **447** (2015) 1847 [https://academic.oup.com/mnras/article-pdf/447/2/1847/8093766/stu2484.pdf].

[22] G. Schönherr, J. Wilms, P. Kretschmar, I. Kreykenbohm, A. Santangelo, R.E. Rothschild et al., *A model for cyclotron resonance scattering features*, *Astron. Astrophys.* **472** (2007) 353 [0707.2105].

[23] W. Coburn, W.A. Heindl, R.E. Rothschild, D.E. Gruber, I. Kreykenbohm, J. Wilms et al., *Magnetic Fields of Accreting X-Ray Pulsars with the Rossi X-Ray Timing Explorer*, *Astrophys. J.* **580** (2002) 394 [astro-ph/0207325].

[24] P.A. Becker and M.T. Wolff, *Thermal and Bulk Comptonization in Accretion-powered X-Ray Pulsars*, *Astrophys. J.* **654** (2007) 435 [astro-ph/0609035].

[25] P. Meszaros, *High-energy radiation from magnetized neutron stars*, University of Chicago Press (1992).

[26] I. Caiazzo and J. Heyl, *Polarization of accreting x-ray pulsars. i. a new model*, *Monthly Notices of the Royal Astronomical Society* **501** (2020) 109 [https://academic.oup.com/mnras/article-pdf/501/1/109/34934429/staa3428.pdf].

[27] J. Poutanen, S.S. Tsygankov and S.V. Forsblom, *X-ray polarimetry of x-ray pulsars*, *Galaxies* **12** (2024) .

[28] P. Meszaros, R. Novick, A. Szentgyorgyi, G.A. Chanan and M.C. Weisskopf, *Astrophysical Implications and Observational Prospects of X-Ray Polarimetry*, *Astrophys. J.* **324** (1988) 1056.

[29] V. Radhakrishnan and D.J. Cooke, *Magnetic Poles and the Polarization Structure of Pulsar Radiation*, *Astrophys. Lett.* **3** (1969) 225.

[30] M.M. Komesaroff, *Possible Mechanism for the Pulsar Radio Emission*, *Nature* **225** (1970) 612.

[31] J. Poutanen, *Relativistic rotating vector model for X-ray millisecond pulsars*, *Astron. Astrophys.* **641** (2020) A166 [2006.10448].

[32] S.S. Tsygankov, V. Doroshenko, J. Poutanen, J. Heyl, A.A. Mushtukov, I. Caiazzo et al., *The x-ray polarimetry view of the accreting pulsar cen x-3*, *The Astrophysical Journal Letters* **941** (2022) L14.

[33] V. Doroshenko, J. Poutanen, S.S. Tsygankov, V.F. Suleimanov, M. Bachetti, I. Caiazzo et al., *Determination of X-ray pulsar geometry with IXPE polarimetry*, *Nature Astronomy* **6** (2022) 1433 [2206.07138].

[34] J. Heyl, V. Doroshenko, D. González-Caniulef, I. Caiazzo, J. Poutanen, A. Mushtukov et al., *X-ray Polarization Reveals the Precessions of the Neutron Star in Hercules X-1*, *arXiv e-prints* (2023) arXiv:2311.03667 [2311.03667].

[35] H.L. Marshall, M. Ng, D. Rogantini, J. Heyl, S.S. Tsygankov, J. Poutanen et al., *Observations of 4U 1626-67 with the Imaging X-Ray Polarimetry Explorer*, *Astrophys. J.* **940** (2022) 70 [2210.03194].

[36] S.V. Forsblom, J. Poutanen, S.S. Tsygankov, M. Bachetti, A.D. Marco, V. Doroshenko et al., *Ixpe observations of the quintessential wind-accreting x-ray pulsar vela x-1*, *The Astrophysical Journal Letters* **947** (2023) L20.

[37] S.S. Tsygankov, V. Doroshenko, A.A. Mushtukov, J. Poutanen, A. Di Marco, J. Heyl et al., *X-ray pulsar GRO J1008−57 as an orthogonal rotator*, *Astron. Astrophys.* **675** (2023) A48 [2302.06680].

[38] C. Malacaria, J. Heyl, V. Doroshenko, S.S. Tsygankov, J. Poutanen, S.V. Forsblom et al., *A polarimetrically oriented X-ray stare at the accreting pulsar EXO 2030+375*, *Astron. Astrophys.* **675** (2023) A29 [2304.00925].

[39] A.A. Mushtukov, S.S. Tsygankov, J. Poutanen, V. Doroshenko, A. Salganik, E. Costa et al., *X-ray polarimetry of x-ray pulsar x persei: another orthogonal rotator?*, *Monthly Notices of the Royal Astronomical Society* **524** (2023) 2004 [https://academic.oup.com/mnras/article-pdf/524/2/2004/54758607/stad1961.pdf].

[40] V.F. Suleimanov, S.V. Forsblom, S.S. Tsygankov, J. Poutanen, V. Doroshenko, R. Doroshenko et al., *X-ray polarimetry of the accreting pulsar GX 301−2*, *Astron. Astrophys.* **678** (2023) A119 [2305.15309].

[41] V. Doroshenko, J. Poutanen, J. Heyl, S.S. Tsygankov, I. Caiazzo, R. Turolla et al., *Complex variations in X-ray polarization in the X-ray pulsar LS V +44 17/RX J0440.9+4431*, *Astron. Astrophys.* **677** (2023) A57 [2306.02116].

[42] J. Poutanen, S.S. Tsygankov, V. Doroshenko, S.V. Forsblom, P. Jenke, P. Kaaret et al., *Studying geometry of the ultraluminous X-ray pulsar Swift J0243.6+6124 using X-ray and optical polarimetry*, *Astron. Astrophys.* **691** (2024) A123 [2405.08107].

[43] S.V. Forsblom, S.S. Tsygankov, J. Poutanen, V. Doroshenko, A.A. Mushtukov, M. Ng et al., *Probing the polarized emission from SMC X-1: The brightest X-ray pulsar observed by IXPE*, *Astron. Astrophys.* **691** (2024) A216 [2406.08988].

[44] Q.C. Zhao, H.C. Li, L. Tao, H. Feng, S.N. Zhang, R. Walter et al., *Polarization perspectives on hercules x-1: further constraining the geometry*, *Monthly Notices of the Royal Astronomical Society* **531** (2024) 3935 [https://academic.oup.com/mnras/article-pdf/531/4/3935/58251747/stae1173.pdf].

[45] D. Kolesnikov, N. Shakura and K. Postnov, *Evidence for neutron star triaxial free precession in her x-1 from fermi/gbm pulse period measurements*, *Monthly Notices of the Royal Astronomical Society* **513** (2022) 3359 [https://academic.oup.com/mnras/article-pdf/513/3/3359/43668332/stac1107.pdf].

[46] P. Reig and P. Roche, *Discovery of two new persistent be/x-ray pulsar systems*, *Monthly Notices of the Royal Astronomical Society* **306** (1999) 100 [https://academic.oup.com/mnras/article-pdf/306/1/100/3459631/306-1-100.pdf].

[47] A. Bahramian and N. Degenaar, *Low-Mass X-ray Binaries*, in *Handbook of X-ray and Gamma-ray Astrophysics*, C. Bambi and A. Santangelo, eds., (Singapore), pp. 1–62, Springer (2023), DOI [2206.10053].

[48] M. van der Klis, *Quasi-periodic oscillations and noise in low-mass X-ray binaries.*, *Annu. Rev. Astron. Astrophys.* **27** (1989) 517.

[49] G. Hasinger and M. van der Klis, *Two patterns of correlated X-ray timing and spectral behaviour in low-mass X-ray binaries.*, *Astron. Astrophys.* **225** (1989) 79.

[50] J. Homan, M. van der Klis, J.K. Fridriksson, R.A. Remillard, R. Wijnands, M. Méndez et al., *XTE J1701-462 and Its Implications for the Nature of Subclasses in Low-magnetic-field Neutron Star Low-mass X-ray Binaries*, *Astrophys. J.* **719** (2010) 201 [1005.3210].

[51] M. Ng, A.K. Hughes, J. Homan, J.M. Miller, S.N. Pike, D. Altamirano et al., *X-Ray and Radio Monitoring of the Neutron Star Low-mass X-Ray Binary 1A 1744-361: Quasiperiodic Oscillations, Transient Ejections, and a Disk Atmosphere*, *Astrophys. J.* **966** (2024) 232 [2310.01511].

[52] A. Papitto, D.F. Torres, N. Rea and T.M. Tauris, *Spin frequency distributions of binary millisecond pulsars*, *Astron. Astrophys.* **566** (2014) A64 [1403.6775].

[53] K. Mitsuda, H. Inoue, K. Koyama, K. Makishima, M. Matsuoka, Y. Ogawara et al., *Energy spectra of low-mass binary X-ray sources observed from Tenma.*, *Publ. Astron. Soc. Jpn.* **36** (1984) 741.

[54] N.I. Shakura and R.A. Sunyaev, *The theory of an accretion disk/ neutron star boundary layer*, *Advances in Space Research* **8** (1988) 135.

[55] R. Popham and R. Sunyaev, *Accretion Disk Boundary Layers around Neutron Stars: X-Ray Production in Low-Mass X-Ray Binaries*, *Astrophys. J.* **547** (2001) 355 [astro-ph/0004017].

[56] N.A. Inogamov and R.A. Sunyaev, *Spread of matter over a neutron-star surface during disk accretion*, *Astronomy Letters* **25** (1999) 269 [astro-ph/9904333].

[57] V. Suleimanov and J. Poutanen, *Spectra of the spreading layers on the neutron star surface and constraints on the neutron star equation of state*, *Mon. Not. R. Astron. Soc.* **369** (2006) 2036 [astro-ph/0601689].

[58] R.A. Syunyaev, V.A. Arefev, K.N. Borozdin, M.R. Gilfanov, V.V. Efremov, A.S. Kaniovskii et al., *Broadband X-Ray Spectra of Black-Hole Candidates X-Ray Pulsars and Low-Mass Binary X-Ray Systems - KVANT Module Results*, *Soviet Astronomy Letters* **17** (1991) 409.

[59] R.M. Ludlam, J.M. Miller, E.M. Cackett, A.C. Fabian, M. Bachetti, M.L. Parker et al., *NuSTAR and XMM-Newton Observations of the Neutron Star X-Ray Binary 1RXS J180408.9-34205*, *Astrophys. J.* **824** (2016) 37 [1604.04252].

[60] A.S. Parikh, R. Wijnands, N. Degenaar, D. Altamirano, A. Patruno, N.V. Gusinskaia et al., *Very hard states in neutron star low-mass X-ray binaries*, *Mon. Not. R. Astron. Soc.* **468** (2017) 3979 [1703.09497].

[61] K. Mitsuda, H. Inoue, N. Nakamura and Y. Tanaka, *Luminosity-related changes of the energy spectrum of X 1608-522.*, *Publ. Astron. Soc. Jpn.* **41** (1989) 97.

[62] N.E. White, L. Stella and A.N. Parmar, *The X-Ray Spectral Properties of Accretion Disks in X-Ray Binaries*, *Astrophys. J.* **324** (1988) 363.

[63] D. Lin, R.A. Remillard and J. Homan, *Evaluating Spectral Models and the X-Ray States of Neutron Star X-Ray Transients*, *Astrophys. J.* **667** (2007) 1073 [astro-ph/0702089].

[64] M. Gilfanov, M. Revnivtsev and S. Molkov, *Boundary layer, accretion disk and X-ray variability in the luminous LMXBs*, *Astron. Astrophys.* **410** (2003) 217 [astro-ph/0207575].

[65] M.G. Revnivtsev and M.R. Gilfanov, *Boundary layer emission and Z-track in the color-color diagram of luminous LMXBs*, *Astron. Astrophys.* **453** (2006) 253 [astro-ph/0506019].

[66] M.G. Revnivtsev, V.F. Suleimanov and J. Poutanen, *On the spreading layer emission in luminous accreting neutron stars*, *Mon. Not. R. Astron. Soc.* **434** (2013) 2355 [1306.6237].

[67] T.R. White, A.P. Lightman and A.A. Zdziarski, *Compton Reflection of Gamma Rays by Cold Electrons*, *Astrophys. J.* **331** (1988) 939.

[68] A.C. Fabian, M.J. Rees, L. Stella and N.E. White, *X-ray fluorescence from the inner disc in Cygnus X-1.*, *Mon. Not. R. Astron. Soc.* **238** (1989) 729.

[69] I.M. George and A.C. Fabian, *X-ray reflection from cold matter in Active Galactic Nuclei and X-ray binaries.*, *Mon. Not. R. Astron. Soc.* **249** (1991) 352.

[70] L. Giridharan, N.T. Thomas, S.B. Gudennavar and S.G. Bubbly, *Spectral and temporal features of GX 13+1 as revealed by AstroSat*, *Mon. Not. R. Astron. Soc.* **527** (2023) 11855 [https://academic.oup.com/mnras/article-pdf/527/4/11855/55375421/stad3941.pdf].

[71] N. Rea, L. Stella, G.L. Israel, G. Matt, S. Zane, A. Segreto et al., *A Compton reflection dominated spectrum in a peculiar accreting neutron star*, *Mon. Not. R. Astron. Soc.* **364** (2005) 1229 [astro-ph/0509692].

[72] J.M. Miller, M.L. Parker, F. Fuerst, M. Bachetti, D. Barret, B.W. Grefenstette et al., *Constraints on the Neutron Star and Inner Accretion Flow in Serpens X-1 Using NuSTAR*, *Astrophys. J. Lett.* **779** (2013) L2 [1310.5776].

[73] G. Risaliti, F.A. Harrison, K.K. Madsen, D.J. Walton, S.E. Boggs, F.E. Christensen et al., *A rapidly spinning supermassive black hole at the centre of NGC 1365*, *Nature* **494** (2013) 449 [1302.7002].

[74] R.M. Ludlam, *Reflecting on accretion in neutron star low-mass X-ray binaries*, *Astrophys. Space Sci.* **369** (2024) 16 [2401.15787].

[75] N. Degenaar, D.R. Ballantyne, T. Belloni, M. Chakraborty, Y.-P. Chen, L. Ji et al., *Accretion Disks and Coronae in the X-Ray Flashlight*, *Space Sci. Rev.* **214** (2018) 15 [1711.06272].

[76] R.A. Sunyaev and L.G. Titarchuk, *Comptonization of low-frequency radiation in accretion disks Angular distribution and polarization of hard radiation*, *Astron. Astrophys.* **143** (1985) 374.

[77] V. Loktev, A. Veledina and J. Poutanen, *Analytical techniques for polarimetric imaging of accretion flows in the Schwarzschild metric*, *Astron. Astrophys.* **660** (2022) A25 [2109.04827].

[78] A. Bobrikova, A. Di Marco, F. La Monaca, J. Poutanen, S.V. Forsblom and V. Loktev, *New polarimetric study of the galactic X-ray burster GX 13+1*, *Astron. Astrophys., in press* (2024) arXiv:2404.01859 [2404.01859].

[79] F. La Monaca, A. Di Marco, J. Poutanen, M. Bachetti, S.E. Motta, A. Papitto et al., *Highly Significant Detection of X-Ray Polarization from the Brightest Accreting Neutron Star Sco X-1*, *Astrophys. J. Lett.* **960** (2024) L11 [2311.06359].

[80] R. Farinelli, S. Fabiani, J. Poutanen, F. Ursini, C. Ferrigno, S. Bianchi et al., *Accretion geometry of the neutron star low mass X-ray binary Cyg X-2 from X-ray polarization measurements*, *Mon. Not. R. Astron. Soc.* **519** (2023) 3681 [2212.13119].

[81] S. Fabiani, F. Capitanio, R. Iaria, J. Poutanen, A. Gnarini, F. Ursini et al., *Discovery of a variable energy-dependent X-ray polarization in the accreting neutron star GX 5−1*, *Astron. Astrophys.* **684** (2024) A137 [2310.06788].

[82] F. Capitanio, S. Fabiani, A. Gnarini, F. Ursini, C. Ferrigno, G. Matt et al., *Polarization Properties of the Weakly Magnetized Neutron Star X-Ray Binary GS 1826-238 in the High Soft State*, *Astrophys. J.* **943** (2023) 129 [2212.12472].

[83] F. Ursini, R. Farinelli, A. Gnarini, J. Poutanen, S. Bianchi, F. Capitanio et al., *X-ray polarimetry and spectroscopy of the neutron star low-mass X-ray binary GX 9+9: An in-depth study with IXPE and NuSTAR*, *Astron. Astrophys.* **676** (2023) A20 [2306.02740].

[84] M.L. Saade, P. Kaaret, A. Gnarini, J. Poutanen, F. Ursini, S. Bianchi et al., *X-Ray Polarimetry of the Dipping Accreting Neutron Star 4U 1624–49*, *Astrophys. J.* **963** (2024) 133 [2312.11655].

[85] A. Di Marco, F. La Monaca, J. Poutanen, T.D. Russell, A. Anitra, R. Farinelli et al., *First Detection of X-Ray Polarization from the Accreting Neutron Star 4U 1820-303*, *Astrophys. J. Lett.* **953** (2023) L22 [2306.08476].

[86] J. Rankin, F. La Monaca, A. Di Marco, J. Poutanen, A. Bobrikova, V. Kravtsov et al., *X-Ray Polarized View of the Accretion Geometry in the X-Ray Binary Circinus X-1*, *Astrophys. J. Lett.* **961** (2024) L8 [2311.04632].

[87] A. Bobrikova, S.V. Forsblom, A. Di Marco, F. La Monaca, J. Poutanen, M. Ng et al., *Discovery of a strong rotation of the X-ray polarization angle in the galactic burster GX 13+1*, *Astron. Astrophys., in press* (2024) arXiv:2401.13058 [2401.13058].

[88] A. Di Marco, F. La Monaca, A. Bobrikova, L. Stella, A. Papitto, J. Poutanen et al., *X-ray Dips and Polarization Angle Swings in GX 13+1*, *arXiv e-prints* (2025) arXiv:2501.05511 [2501.05511].

[89] M. Cocchi, A. Gnarini, S. Fabiani, F. Ursini, J. Poutanen, F. Capitanio et al., *Discovery of strongly variable X-ray polarization in the neutron star low-mass X-ray binary transient XTE J1701−462*, *Astron. Astrophys.* **674** (2023) L10 [2306.10965].

[90] R.E. Spencer, A.P. Rushton, M. Bałucińska-Church, Z. Paragi, N.S. Schulz, J. Wilms et al., *Radio and X-ray observations of jet ejection in Cygnus X-2*, *Mon. Not. R. Astron. Soc.* **435** (2013) L48 [1306.0599].

[91] Q. Zhao, H. Li, L. Tao and H. Feng, *Discovery of Rapid Polarization Angle Variation During the 2022 Outburst of XTE J1701-462*, *arXiv e-prints* (2024) arXiv:2411.11352 [2411.11352].

[92] A. Di Marco and IXPE Science Team, *Weakly magnetized accreting neutron stars as seen by ixpe*, *Astronomische Nachrichten* (2024) e20240126 [https://onlinelibrary.wiley.com/doi/pdf/10.1002/asna.20240126].

[93] E.B. Fomalont, B.J. Geldzahler and C.F. Bradshaw, *Scorpius X-1: The Evolution and Nature of the Twin Compact Radio Lobes*, *Astrophys. J.* **558** (2001) 283 [astro-ph/0104372].

[94] K.S. Long, G.A. Chanan, W.H.M. Ku and R. Novick, *The linear X-ray polarization of Scorpius X-1.*, *Astrophys. J. Lett.* **232** (1979) L107.

[95] X. Long, H. Feng, H. Li, J. Zhu, Q. Wu, J. Huang et al., *A Significant Detection of X-ray Polarization in Sco X-1 with PolarLight and Constraints on the Corona Geometry*, *Astrophys. J. Lett.* **924** (2022) L13 [2112.02837].

[96] J. Poutanen, A. Veledina and A.M. Beloborodov, *Polarized X-Rays from Windy Accretion in Cygnus X-1*, *Astrophys. J. Lett.* **949** (2023) L10 [2302.11674].

[97] A.F. Tennant, A.C. Fabian and R.A. Shafer, *Observations of type I X-ray bursts from CIR X-1.*, *Mon. Not. R. Astron. Soc.* **221** (1986) 27P.

[98] H.M. Johnston, R. Fender and K. Wu, *High-resolution optical and infrared spectroscopic observations of CIR X-1*, *Mon. Not. R. Astron. Soc.* **308** (1999) 415 [astro-ph/9904112].

[99] N.S. Schulz, T.E. Kallman, S. Heinz, P. Sell, P. Jonker and W.N. Brandt, *The young Be-star binary Circinus X-1*, *IAU Symposium* **346** (2019) 125.

[100] S. Heinz, N.S. Schulz, W.N. Brandt and D.K. Galloway, *Evidence of a Parsec-Scale X-Ray Jet from the Accreting Neutron Star Circinus X-1*, *Astrophys. J. Lett.* **663** (2007) L93 [0706.3881].

[101] P. Soleri, S. Heinz, R. Fender, R. Wijnands, V. Tudose, D. Altamirano et al., *A parsec scale X-ray extended structure from the X-ray binary Circinus X-1*, *Mon. Not. R. Astron. Soc.* **397** (2009) L1 [0810.2202].

[102] S.W. Davis and A. Tchekhovskoy, *Magnetohydrodynamics Simulations of Active Galactic Nucleus Disks and Jets*, *Annu. Rev. Astron. Astrophys.* **58** (2020) 407 [2101.08839].

[103] F. Cowie, R. Fender and I. Heywood, *Circinus X-1: Powerful relativistic jets from a neutron star*, *contributed talk, EAS2024 Annual Meeting* (2024) id.662.

[104] R. Iaria, T. Di Salvo, L. Burderi, A. Riggio, A. D'Aì and N.R. Robba, *Discovery of periodic dips in the light curve of GX 13+1: the X-ray orbital ephemeris of the source*, *Astron. Astrophys.* **561** (2014) A99 [1310.6628].

[105] A. D'Aì, R. Iaria, T. Di Salvo, A. Riggio, L. Burderi and N.R. Robba, *Chandra X-ray spectroscopy of a clear dip in GX 13+1*, *Astron. Astrophys.* **564** (2014) A62 [1403.0071].

[106] M. Diaz Trigo, L. Sidoli, A. Parmar and L. Boirin, *Is GX 13+1 a dipping source?*, in *X-ray Astronomy 2009; Present Status, Multi-Wavelength Approach and Future Perspectives*, A. Comastri, L. Angelini and M. Cappi, eds., vol. 1248 of *AIP Conf. Ser.*, pp. 153–154, AIP, July, 2010, DOI.